SEARCH FOR THE QUARK-GLUON PLASMA — THE NA35 EXPERIMENT AT THE CERN SPS*

By H. G. Pugh**

Lawrence Berkeley Laboratory, University of California, Berkeley, CA 94120, U.S.A. and the NA35 Collaboration

(Received September 7, 1987)

In 1986, a new era of studies of nucleus-nucleus collisions was ushered in when CERN accelerated ^{16}O nuclei to energies of 60 GeV/nucleon and 200 GeV/nucleon for a series of experiments with nuclear targets. In this paper, some preliminary results are presented from the NA35 experiment, which uses a Streamer Chamber in conjunction with extensive hadronic and electromagnetic calorimetry. Evidence is found for production of energy densities in the interaction volume comparable to those predicted to be sufficient for formation of a quark-gluon plasma. Many of the early results can be understood in terms of simple extrapolation from nucleon-nucleon and/or nucleon-nucleus interactions. Areas where such a simple interpretation does not seem to apply are mentioned.

PACS numbers: 12.38.Mh

1. Introduction

Collisions of nuclei at very high energy should create a finite volume of hadronic matter at high energy density. Recent results from strong interaction lattice gauge theory [1] suggest that, above a critical temperature of approximately 250 MeV, the hadronic state of matter is transformed to a new phase consisting of deconfined quarks and gluons with an energy density of a few GeV/fm^3, to be compared with that of ground state matter which is 150 MeV/fm^3. Such extreme conditions could be reached in central nucleus-nucleus collisions by converting the initial relative c.m. energy into internal excitation of a 'fireball' formed at rapidities intermediate between those of target and projectile, provided sufficient beam energy and adequate 'stopping power'.

The goal of the CERN SPS experiment NA35 is to explore the properties of nucleus-nucleus collisions at 60 and 200 GeV/nucleon, to learn about the degree of stopping and thermalization, and energy densities achievable in such collisions, and to measure

* Presented at the XXVII Cracow School of Theoretical Physics, Zakopane, Poland, June 3–15, 1987.

** Recipient of a U.S. Senior Scientist Award from the Alexander von Humboldt Foundation, as a guest of the University of Frankfurt.

other quantities related to them. Here we present preliminary results from the 1986 running period, in which beams of ^{16}O ions at 60 and 200 GeV/nucleon were used, as well as beams of protons and π^+ at 200 GeV for comparison. A second run with ^{32}S projectiles is scheduled for September, 1987.

2. Experimental set-up

Figure 1 shows the NA35 experimental set-up. The main components are [2]:

A. A large-volume Streamer Chamber, $2 \times 1.2 \times 0.7\ m^3$, in a 1.5 T superconducting vertex magnet. Targets of Al, Cu, Ag, Au, and Pb, of 1% interaction length thickness (and also 0.2% for Au) were mounted directly in front of the chamber. Two principal readout systems were employed:

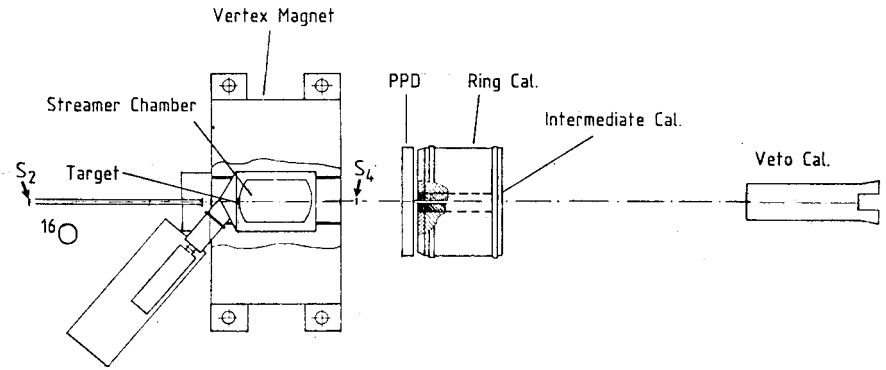

Fig. 1. The NA35 experimental set-up

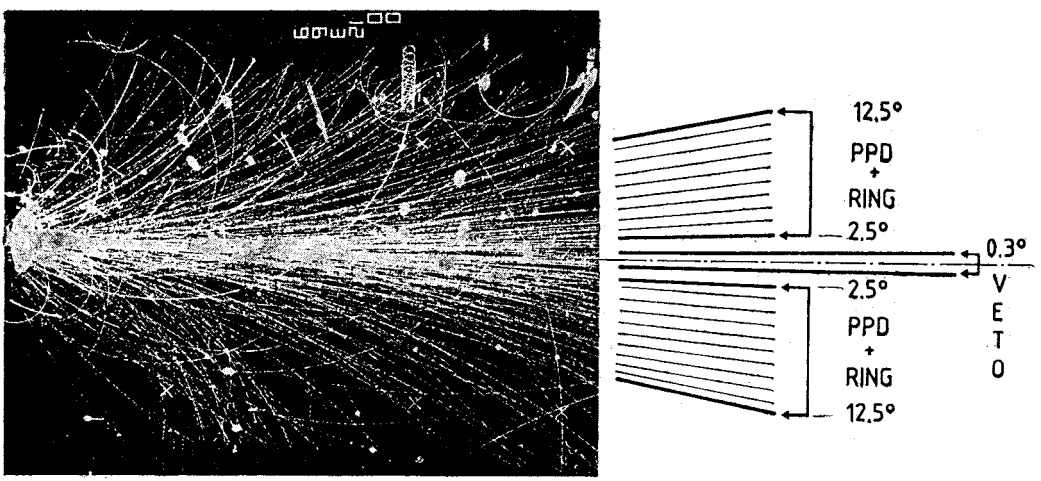

Fig. 2. Streamer Chamber picture of a central ^{16}O + Pb collision at 200 GeV/nucleon, together with the angular acceptance of the mid-rapidity calorimeters (PPD and ring) and the leading fragment calorimeter (Veto)

a. A set of 3 film cameras with Zeiss optics recorded on high-sensitivity 70 mm film. They were equipped with two-stage magnetic-focusing ITT image intensifiers of about 2500-fold gain. The spatial resolution was of the order of 2 mm. The film is analyzed off line at the CERN Bessymatic and ERASME facilities, as well as in Berkeley, Cracow, Frankfurt, Heidelberg, Marburg, München, Warsaw, and Zagreb. A typical central ^{16}O + Pb event at 200 GeV/A is shown in Fig. 2.

b. Two CCD digitizing cameras, with TI 1024 × 1024 byte arrays and equipped with two stages of image intensifiers, recorded the events on line. With the help of a micro-VAX based image processing and display system, events were monitored, and the multiplicity of charged tracks obtained on line [3].

B. A set of electromagnetic and hadronic calorimeters. The angular domain $\theta < 0.3°$ (nuclear projectile fragmentation) is covered by a 4-segment "Veto" Calorimeter. The subsequent interval, 0.3°–2.2°, has a continuous single-cell EM + hadronic calorimeter. The larger angle domain is covered in high granularity by a Photon Position Detector (PPD) consisting of alternating layers of lead and planes of proportional tubes read out by 3072 ADC channels, and by a Ring Calorimeter divided into 240 cells (24 in azimuth and 10 in radius with sizes chosen to cover equal units of rapidity).

This set of calorimeters is movable: at 200 GeV/nucleon it covered a 2.3°–12.5° angular range corresponding to $2.2 < y < 3.8$, and at 60 GeV/nucleon it covered a 4.3°–20.5° range corresponding to $1.7 < y < 3.3$. Some measurements were also made with other settings.

Two principal trigger modes were employed. From the Veto Calorimeter various levels of projectile energy degradation could be selected, ranging from "minimum bias" to "central collision", the latter requiring $E_{veto} < 0.1\, E_{beam}$. The other trigger was obtained from the transverse energy of the produced photons, recorded in the PPD. On the average 3 Streamer Chamber events were recorded per extraction spill, and in addition about 100 events in the calorimeters without accompanying streamer chamber information. At incident energies of 60 and 200 GeV/nucleon, a total of about 100,000 Streamer Chamber and 2,500,000 calorimeter events were recorded. In addition, data were taken for 200 GeV incident protons and π^+. Data analysis is in progress. First results on multiplicity and transverse energy distributions have been published [4].

3. Experimental results

3.1. Total inelastic cross-section

The total inelastic cross sections have been extracted for interactions of the 200 GeV/nucleon ^{16}O beam with two targets (Cu and Au) and also for interactions with the Streamer Chamber gases (He and Ne). Only events with at least two secondary tracks seen in the Streamer Chamber have been used in the cross section determination. In Fig. 3 a comparison is made with values for various projectile target combinations studied at significantly lower energies, at the Bevalac and Synchrophasotron [5]. The cross sections obtained for ^{16}O-He, ^{16}O-Ne and ^{16}O-Au interactions at 60 GeV/nucleon (not shown)

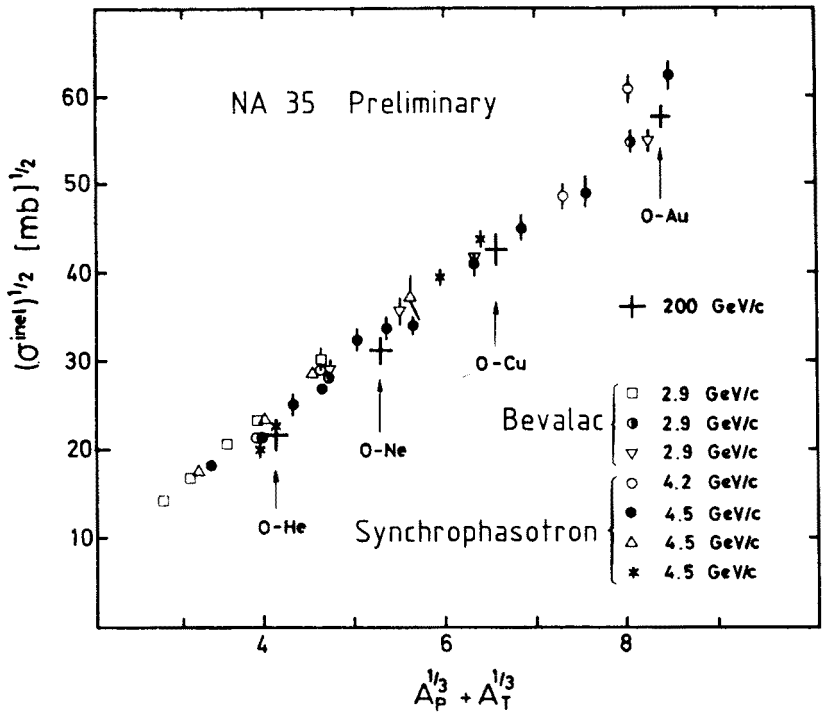

Fig. 3. The total inelastic cross section for the interaction of 200 GeV/nucleon ^{16}O with four targets, and for a variety of projectile-target combinations at the Bevalac and Synchrophasotron. The axes are chosen to emphasize the geometrical origin of these cross sections

agree within statistical errors with the 200 GeV/nucleon data. We conclude that the general dependence of σ_{inel} on A_p and A_T at 60 and 200 GeV/nucleon is mainly determined by geometrical factors and is independent of the projectile energy.

3.2. Energy loss spectrum

The "veto" calorimeter, which subtends an angle of 0–0.3° in the forward direction, is designed to measure the energy contained in that part of the projectile which does not interact strongly with the target nucleus. Thus, in a peripheral collision, part of the projectile will overlap with the target nucleus and will interact violently with reaction products generally appearing at angles outside the acceptance of the veto calorimeter, while the remainder of the projectile will continue on as one or more nuclear fragments all with the same velocity as the beam except for the addition of a small amount of "fermi" motion. Since all the nuclear fragments would be captured by the veto calorimeter, its signal will be proportional to the number of non-interacting nucleons and provide a measure of the impact parameter in the collision. Fig. 4 shows the observed spectra for a gold target at 200 GeV/nucleon and at 60 GeV/nucleon. It is clear that at each energy there is a substantial yield with $E_{veto} \approx 0$, corresponding to head-on collisions with no nuclear projectile fragments. This condition has been used to select such interactions.

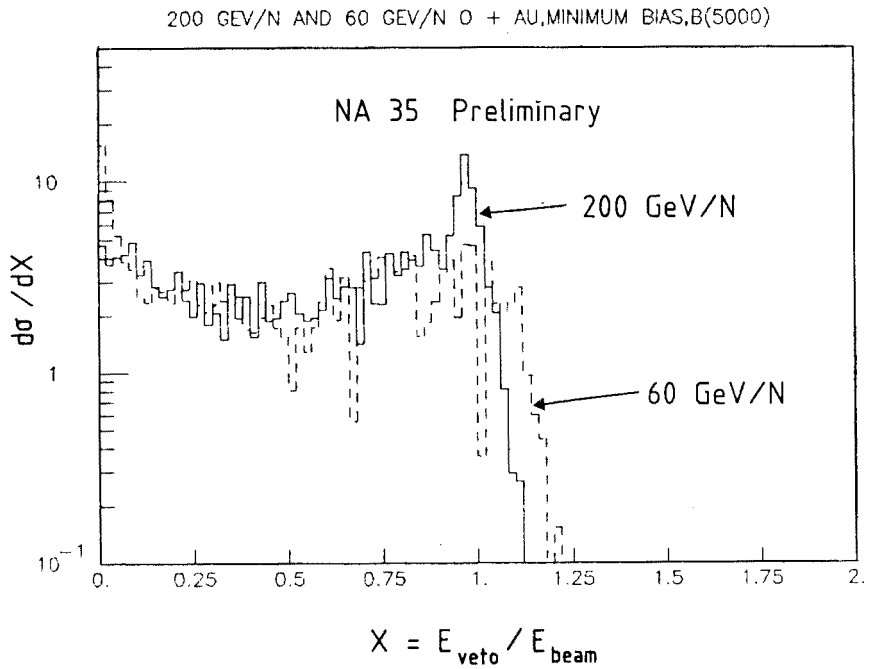

Fig. 4. The energy spectrum in the Veto Calorimeter for ^{16}O + Au at 200 GeV/nucleon and 60 GeV/nucleon, plotted as a function of the parameter $X = E_{veto}/E_{beam}$

Such spectra contain some information on the "stopping power" of nuclei, which is of great interest to determine the optimum conditions for producing high energy densities. However, since the qualitative features of the spectrum are dominated by simple geometric considerations, the extraction of such information will be difficult.

3.3. Charged particle multiplicities

The charged particle multiplicity at laboratory angles $\theta < 60°$ was obtained from a double scan of the Streamer Chamber pictures, corrections being made for scanning efficiency, e^+e^- contamination from π^0 conversion, secondary interactions in the target, and contributions from neutral strange particle decays into charged particles (based on the HIJET prediction for the relative Λ, K_s^0, Σ, and pion yields). Fig. 5 shows the results for ^{16}O + Pb at 200 GeV/nucleon, plotted as a function of the total energy in the veto calorimeter. The mean charged multiplicity increases, with decreasing energy in the (nuclear) fragmentation domain. This finding can be related to two different processes which are well known from hadron-nucleus and low energy nucleus-nucleus interactions: the increase of the particle multiplicity is due to (*i*) the increase of the number of participants from the projectile nucleus, and (*ii*) the increase of the particle production per participating projectile nucleon with increasing thickness of the target nuclear matter. Both effects are taken into account in the HIJET model [6], whose predictions are also shown in the figure. This model uses a simple geometrical picture of nucleus-nucleus collisions and assumes that

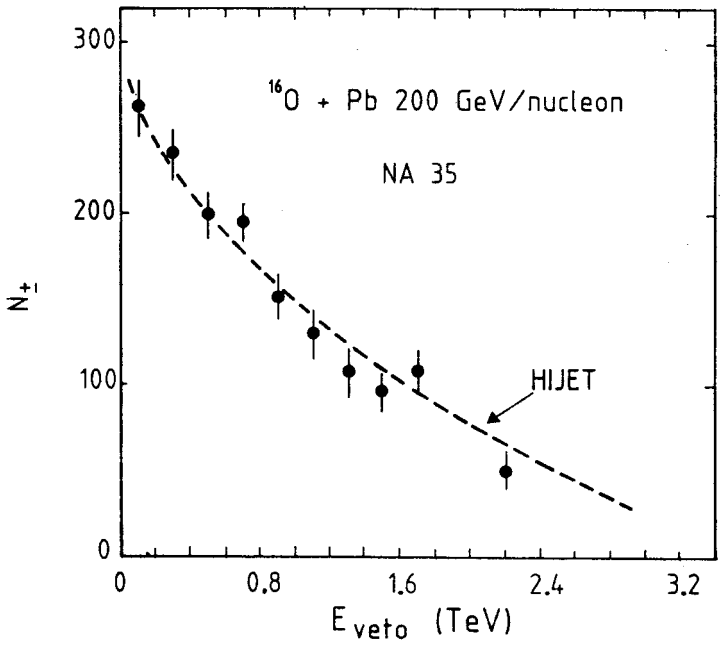

Fig. 5. Mean charged particle multiplicity for laboratory angles $\theta < 60°$ as a function of the total energy observed in the Veto Calorimeter

only the leading baryons cascade. HIJET is based on the program ISAJET, constructed to fit measured pp and $\bar{p}p$ data, and is known to predict correctly the multiplicities in p-nucleus collisions [4].

The mean charged multiplicity for central collisions ($E_{veto} \sim 0$) is about 260. At 60 GeV/nucleon the corresponding figure is about 190. At each energy the excess of positive over negative particles is found, in central collisions, to be about 30. The interpretation of these numbers is as follows: the charged particles can be classified as (1) produced particles, with approximately equal numbers of each sign (not exactly, since the isospin of the target is not zero), (2) target spectators, most of which fall outside the acceptance of the streamer chamber, (3) projectile spectators, of which there should be none for the central collisions being considered, and (4) participant protons, deuterons, or heavier nuclear fragments. According to this rough classification, the number of participant protons in central ^{16}O + Pb collisions is about 30. This is consistent with the 16 nucleons of the projectile striking a cylinder of about 50 target nucleons.

3.4. Transverse energy distribution

Figure 6 shows the differential transverse energy (E_T) distribution for ^{16}O + Pb at 200 GeV/nucleon, as summed from the PPD and Ring calorimeters, with the magnetic field off. The value of E_T is calculated for each event as the appropriately weighted sum of the energies found in individual PPD and Ring Calorimeter channels. For the data points with $E_T < 50$ GeV the streamer chamber was used to verify that each of the included

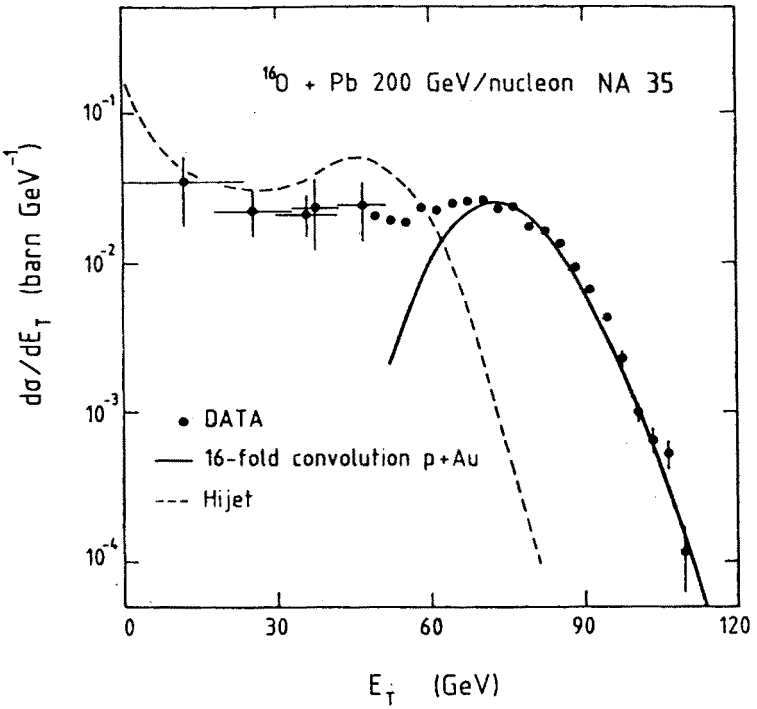

Fig. 6. Mid rapidity transverse energy distribution for ^{16}O + Pb at 200 GeV/nucleon. The dashed curve gives the HIJET prediction. The full line is a 16-fold convolution of the E_T distribution for inelastic p + Au collisions at 200 GeV, measured with the same apparatus

events was a valid target interaction. For $E_T > 50$ GeV the fraction of non-target interactions was less than 4%. Systematic uncertainties in the E_T scale and normalization are estimated to be about 10%. The range of rapidities included in the data is approximately $2.2 < y < 3.8$.

The HIJET prediction is also shown in Fig. 6 for comparison. This distribution is much narrower. The peak near 50 GeV arises in this model from impact parameters $b < 4$ fm. The data exhibit the same "central collision" peak at around 75 GeV. The total observed cross section for $E_T > 75$ GeV is 250 mb, corresponding in a geometric model to $b \leqslant 3$ fm. The yield is still appreciable at a value of E_T of 110 GeV, or 1.5 times the average value for central collisions.

3.5. Dependence of E_T on A_p

In order to understand the E_T spectrum further, the same measurement was made for p + Au, using a tagged 200 GeV proton beam. To eliminate surface interactions the value of E_{veto} was required to be less than 150 GeV, corresponding to a p-Au cross section of 1.3 barns, or impact parameters $b < 6$ fm. The result is shown in Fig. 7, along with an analytic fit $d\sigma/dE_T = 0.173\, E_T^{2.36} \exp(-0.727\, E_T)$ barn/GeV, and a HIJET prediction for $b < 6$ fm. The HIJET model yields too low values of E_T. A 16-fold convolution of

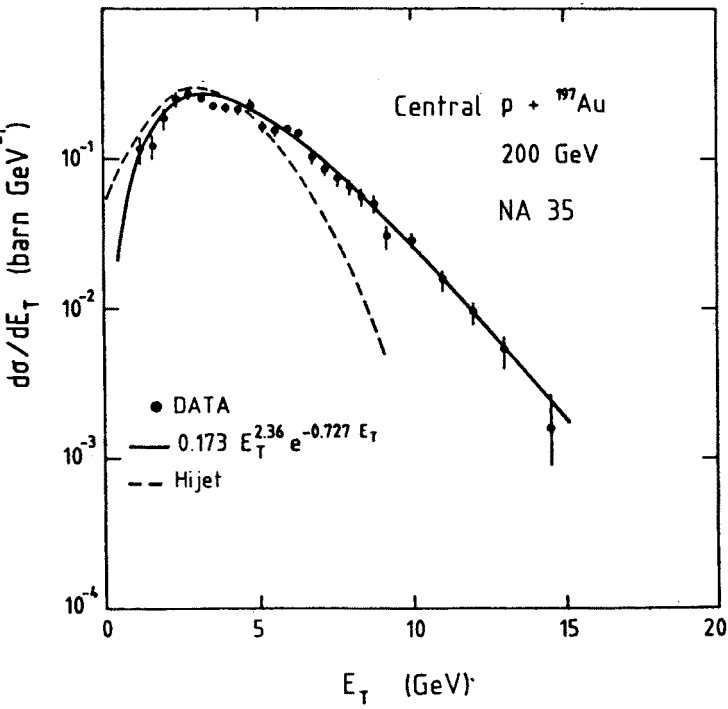

Fig. 7. Mid rapidity transverse energy distribution for central p + Au at 200 GeV. The dashed curve gives the HIJET prediction for b < 6fm, and the full line is a functional fit to the data

the p + Au data is shown in Fig. 6, where it provides an excellent fit to the "central collision" peak, both as regards position and shape at high E_T. The difference between Au and Pb for the purposes of this convolution is not expected to be significant. The Gaussian shape of the "central collision" peak is a result of the central limit theorem. The failure of the HIJET calculation to fit the ^{16}O + Pb data is clearly due to its failure to predict sufficient E_T in the p-nucleus collisions.

This result implies that the value of E_T for central collisions is proportional to the number of nucleons in the projectile, A_p, provided that the projectile is small compared with the target nucleus.

3.6. Dependence of E_T on beam energy

Figure 8 shows the E_T spectra measured for ^{16}O + Au at 60 GeV/nucleon ($2.0 < y < 3.5$) and at 200 GeV/nucleon ($2.2 < y < 3.8$). The energy calibration is revised upwards from that of Figs 6, 7, but is still preliminary. The mean E_T for central collisions is approximately 45 and 90 GeV at 60 and 200 GeV/nucleon respectively.

To estimate what values we might expect, we consider the total c.m. energy available ($\sqrt{s}$) in the 16+50 system consisting of the projectile nucleus and the tube of participant nucleons in the target nucleus. This is 318 and 582 GeV respectively. An upper limit for E_T might be the value for an isotropic fireball, i.e., $\pi/4 \times E_{cm}$: 250 GeV and 457 GeV respec-

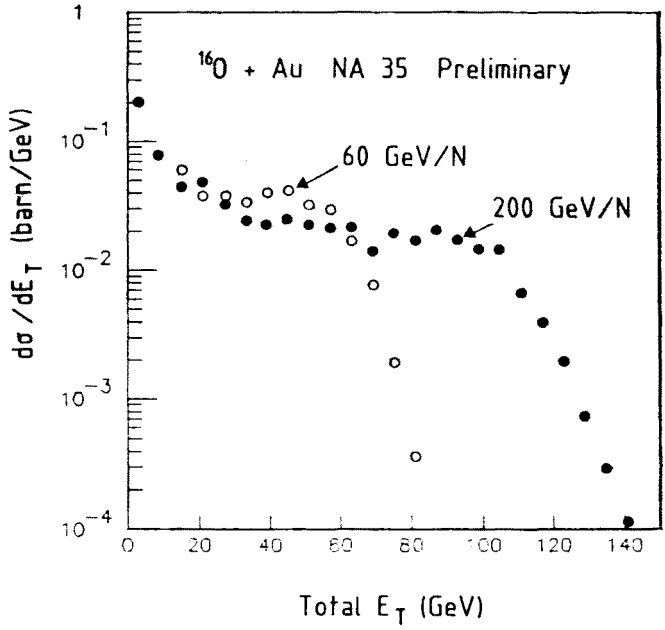

Fig. 8. Mid rapidity transverse energy distributions for ^{16}O + Au at 60 GeV/nucleon ($2.0 < y < 3.5$) and at 200 GeV/nucleon ($2.2 < y < 3.8$). The energy calibration (still preliminary) has been revised upwards compared with that used for Figs 6, 7

tively. Since the experimental acceptance is about one half, these values would be reduced to 125 GeV and 229 GeV. The average E_T for central collisions is therefore, at both energies, about 40% of the value for an isotropic fireball. It is also interesting to note that the observed E_T is approximately proportional to $\sqrt{s}$.

3.7. Estimates of energy density

From the E_T measurements we can make an estimate of the energy density in the interaction volume, using the formula of Bjorken [7].

$$\varepsilon_t \sim \frac{\Delta E_T}{\Delta y} \Big/ (\pi r^2 \tau),$$

where ΔE_T is the transverse energy observed in the rapidity interval y, r is the radius of the ^{16}O nucleus and τ is the time that has elapsed since the beginning of the collision. For $\tau = 1$ fm/c, and the observed $\Delta E_T = 90$ GeV in $2.2 < y < 3.8$ at 200 GeV/nucleon, we find an energy density of 2.0 GeV/fm^3. We can make a similar estimate for the rapidity interval $0.6 < y < 2.4$ by using the E_T distribution for p + Pb at 200 GeV measured by the CERN NA34 collaboration [8]. Applying a 16-fold convolution to those data we find $\Delta E_T = 125$ GeV over $\Delta y = 1.8$, yielding an energy density of 2.5 GeV/fm^3. We conclude that the energy density reached in ^{16}O + Au collisions at 200 GeV/nucleon is of the order of 2 GeV/fm^3. At 60 GeV/nucleon it is about half as great.

The energy density at 200 GeV/nucleon is comparable with the values that have been suggested for formation of a quark-gluon plasma, justifying an intensive search at this energy. To obtain higher values, three avenues appear open:

A. Select events with unusually high E_T, on the tail of the distribution. This could increase the energy density by a factor of 1.5 while still providing a useful yield.

B. Use projectiles with greater mass. Here we expect E_T to be proportional to A_p (from A-fold convolution) while the interaction volume only increases as $A_p^{2/3}$ for a net $A_p^{1/3}$ dependence.

C. Use higher beam energies, since the transverse energy seems to be proportional to $\sqrt{s}$.

It should be remarked, however, that the expression used for the energy density is very schematic, and at present has only qualitative utility.

3.8. Dependence of E_T on A_t

Figure 9 shows the transverse energy spectrum measured in the PPD (which is sensitive primarily to the electromagnetic component) for various targets at 200 GeV/nucleon. In the Au spectra the "central collision peak" is not so evident as in Figs 7, 8 because its width

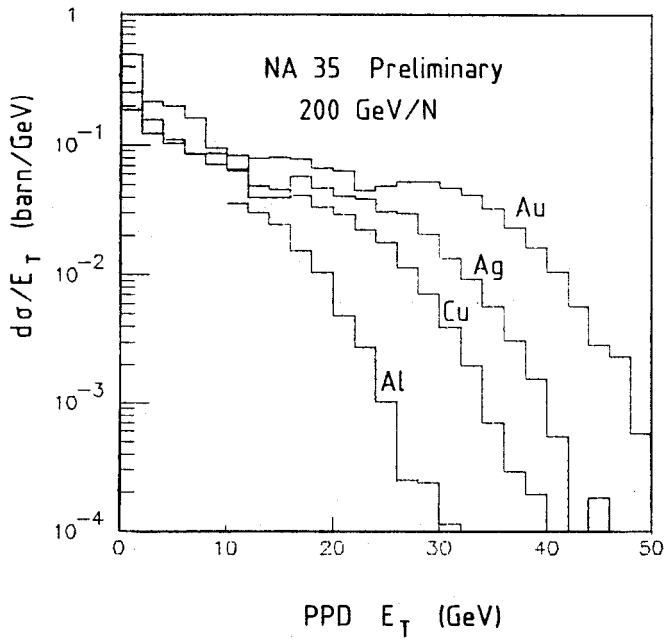

Fig. 9. Transverse component of the deposition of electromagnetic energy in the PPD for ^{16}O + Al, Cu, Ag, Au, at 200 GeV/nucleon

is relatively greater than in the complete E_T measurement. For the lighter nuclei this effect is compounded by the fact that central collisions form a smaller fraction of the total than for Au. Because of these effects detailed calculations will be needed to explain these spectra. However, a preliminary analysis indicates that, when the projectile is small compared with

the target nucleus (i.e., excluding Al from the present data set) the mean electromagnetic E_T for central collisions is proportional to $A_t^{1/3}$.

This $A_t^{1/3}$ dependence is consistent with E_T being proportional to the number of nucleon-nucleon collisions taking place in the interaction, a result which was implied already by the proportionality of E_T to A_p. A corollary is that E_T is not proportional to $\sqrt{s}$ as A_t is increased since that would increase as $A_t^{1/6}$.

3.9. Rapidity distributions

We now turn to the information (other than multiplicities) that can be extracted from the Streamer Chamber photographs. Here we measure the charge and momentum of each of the individual charged particles, as well as of neutral particles which have a charged decay mode. At present a few hundred central (low E_{veto} and/or high E_T) events have been fully measured, yielding several tens of thousands of measured tracks. For the preliminary results shown here, all the negative charged particles are assumed to be pions.

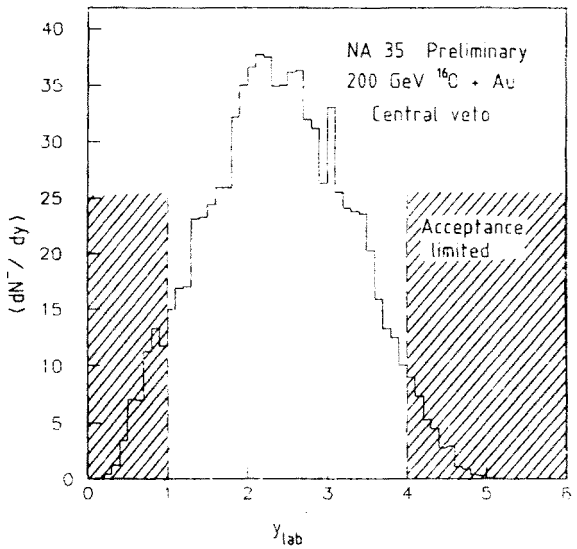

Fig. 10. Rapidity distribution for negatively charged particles, assumed to be pions, for ^{16}O + Au central collisions at 200 GeV/nucleon. The shaded areas indicate those parts of the distribution which were not used in the analysis described in Section 3.13. No corrections for acceptance have been made: such corrections are expected to increase dN/dy by about 20% at the peak

Figure 10 shows the rapidity distribution for ^{16}O + Au central collisions at 200 GeV/nucleon. While the data still have to be corrected for acceptance, we can clearly see that the distribution is not centered on the value expected for free nucleon-nucleon collisions, i.e., $y = 3.03$. The value $y = 2.46$ which corresponds to the c.m. of 16+50 nucleons, seems to be more appropriate.

3.10. Center of mass angular distributions

The width of the rapidity distribution shown in Fig. 10 is too great to be attributable to isotropic particle emission, as was foreseen by our discussion of the E_T spectra. In order to quantify this, $\langle \cos^2 \theta \rangle^{1/2}$ was calculated for the negatively charged particles at 60 GeV/nucleon, where θ is the particle emission angle in the c.m. frame (chosen to minimize the above quantity). The value was found to be 0.70, larger than the value of 0.577 expected for an isotropic distribution, but significantly lower than the value of 0.75 ± 0.02 for p-p collisions at the same energy [9]. This is consistent with the fact that the rapidity distribution is narrower than that for p-p collisions.

3.11. Average transverse momentum

The average transverse momentum per particle is a quantity that can be determined from a small subsample of events, since the number of particles per event is high. Preliminary values for $\langle p_T \rangle$ for negative particles from central ^{16}O + Au collisions are 320 ± 20 and 325 ± 20 MeV/c at 60 GeV/nucleon and 200 GeV/nucleon respectively. No corrections have been applied, but the corrections are not expected to be greater than 10%. These results are shown in Fig. 12, together with previous results for pions produced in nucleon-

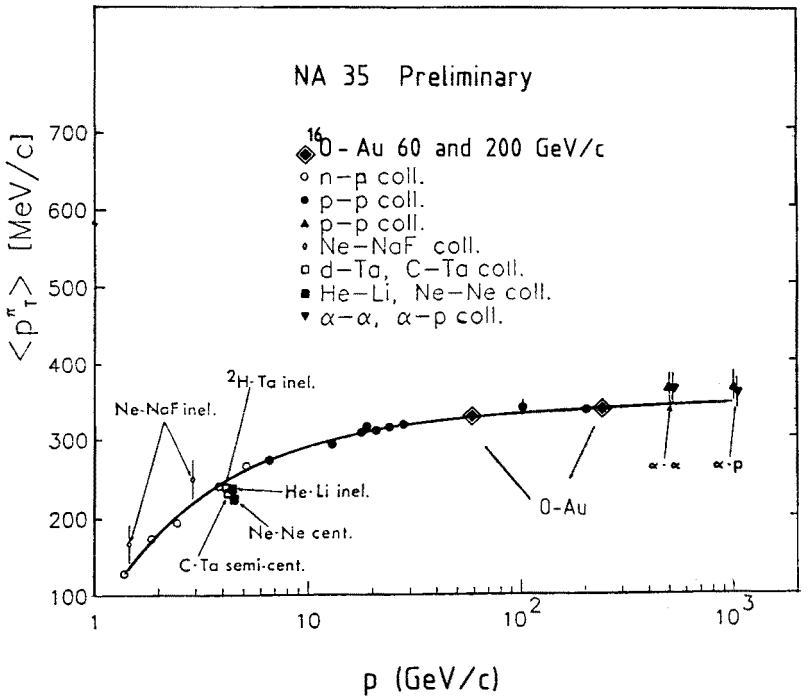

Fig. 11. The mean transverse momentum observed for pions produced in nucleon-nucleon and nucleus--nucleus collisions as a function of the incident beam momentum per nucleon. The points from NA35 represent preliminary value of $\langle p_T \rangle$ for negative pions. The line represents the trend of the nucleon-nucleon data

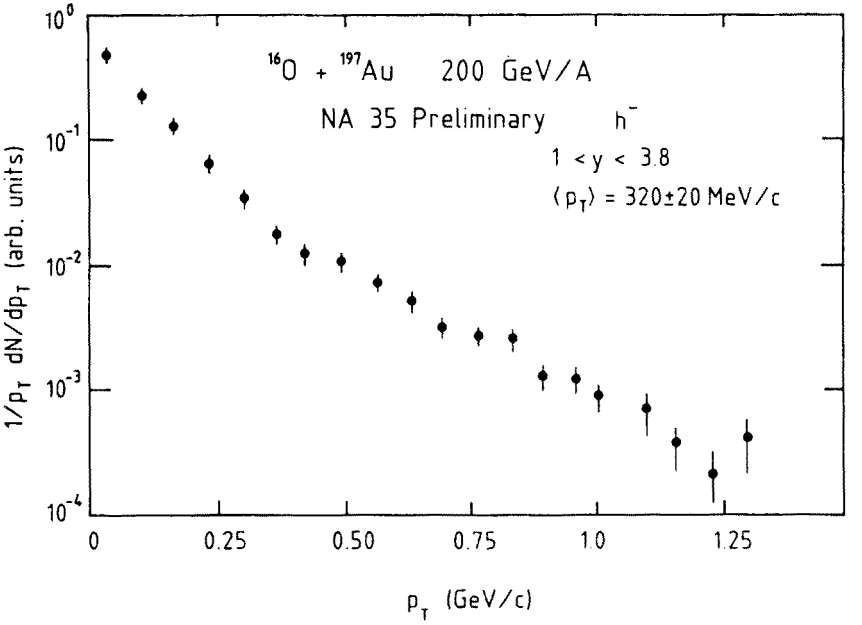

Fig. 12. Transverse momentum distribution for negatively charged particles with $1.0 < y < 3.8$ for central ^{16}O + Au collisions at 200 GeV/nucleon. No corrections have yet been applied to these data

-nucleon and nucleus-nucleus collisions. They are consistent with the trend of the other data, and with the values observed in nucleon-nucleon collisions.

3.12. Transverse momentum distribution

The transverse momentum distributions are much more sensitive to systematic errors than the mean presented above, and also require better statistics for their determination. We present in Fig. 13 the transverse momentum distribution for negative particles at $1.0 < y < 3.8$ for a sample of central ^{16}O + Au collisions at 200 GeV/nucleon. Corrections still have to be made, especially for electrons produced from π^0 decay and γ conversion to the target, which are most important at low p_T. The mean transverse momentum per particle is 320 ± 20 MeV/c for this sample.

The results in Fig. 13 appear to show a non-exponential shape. This is a surprise, since none of the models based on nucleon-nucleon collisions (e.g., HIJET, the Lund model, etc.) show other than a single component at these values of p_T. If the spectrum is fitted with two sources in a thermal model, the sources are found to make roughly equal contributions, with temperatures of about 60 and 180 MeV respectively. A statistical analysis of these data on an event-by-event basis shows clearly that the two-component structure is not due to two different types of event — hot and cold. Both components are present in all events. At this stage of the data analysis it is too early to speculate on the explanation of this result. There is some evidence for a similar effect in cosmic ray data [10], where a combination of thermal excitation and radial flow was suggested to explain the observations.

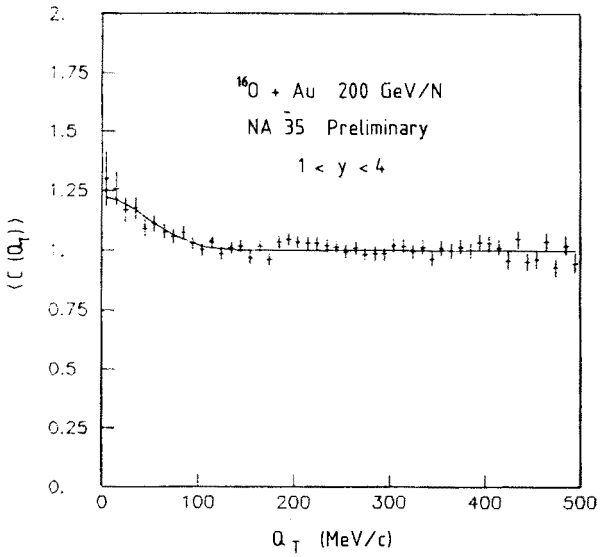

Fig. 13. The 2-pion correlation function projected on to the $Q_\perp$ axis, for pairs in which Q_0, $Q_{11} \leqslant 100$ MeV/c, in ^{16}O + Au central collisions at 200 GeV/nucleon, for pions with $1 < y < 4$

3.13. Two-pion correlation

The Streamer Chamber technique is particularly attractive for pion-interferometric studies in a high multiplicity interaction. By virtue of the "4π" geometry, 105 central ^{16}O-Au interactions at 200 GeV/nucleon (referred to above) yield about 420,000 negative particle pairs.

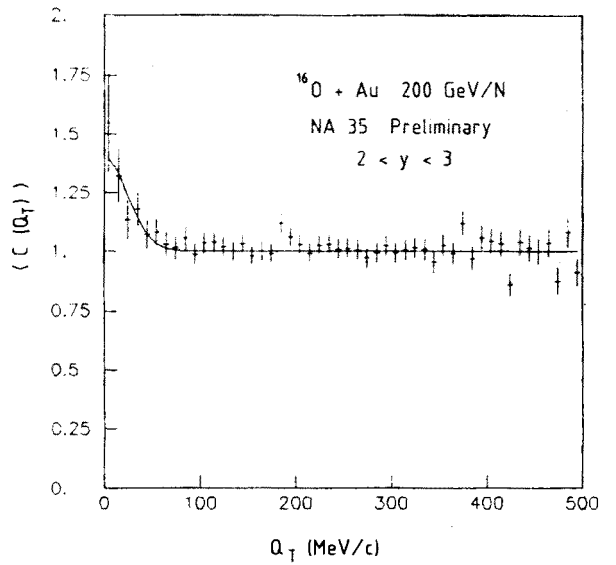

Fig. 14. The same as Fig. 13, but for pions with $2 < y < 3$

In the analysis of those pairs (all assumed to be negative pions) a correlation function

$$C(Q_\perp, Q_\parallel) \propto 1+\lambda \exp(-Q_\perp^2 R_\perp^2/2 - Q_\parallel^2 R_\parallel^2/2)$$

was assumed, where $Q_\perp$ is the momentum difference between the two pions in the transverse direction, and $Q_\parallel$ is the momentum difference in the longitudinal direction, both calculated in the "16+50" c.m. frame. The quantity λ is the coherence parameter, while $R_\perp$ and $R_\parallel$ are transverse and longitudinal radius parameters. Figs 13 and 14 show the correlation function projected on to the $Q_\perp$ axis, for Q_0, $Q_\parallel$, $\leqslant 100$ MeV/c, for pions in the rapidity intervals $1 < y < 4$ and $2 < y < 3$ respectively. The extracted parameter values are given in Table I.

TABLE I

Parameter values extracted from the 2-pion correlation analysis (preliminary)

y range	$R_\perp$ (fm)	$R_\parallel$ (fm)	λ	No. of pairs
1.0–4.0	$4.1^{+0.5}_{-0.4}$	$3.1^{+0.7}_{-0.3}$	$0.31^{+0.07}_{-0.03}$	204,000
2.0–3.0	8.1 ± 1.6	$5.6^{+1.2}_{-0.8}$	0.77 ± 0.19	39,000

From Table I we see that the pion source has a tendency to oblateness with respect to the beam axis. In measurements of p-p and α-α collisions at the ISR [11], the pion source was found to be prolate for p-p collisions and spherical for α-α collisions. See also Ref. [12]. When pions in the rapidity range y = 2.0–3.0 are selected, we find a marked increase in the size of the source and of the chaoticity parameter λ. This suggests the formation of a thermalized fireball at mid-rapidity for the 16+50 system, superimposed on a more coherent source over a wider rapidity interval.

4. Summary and conclusions

A new frontier in nucleus-nucleus collisions has been opened to systematic study; and the major features of the new landscape are beginning to be mapped out.

While most of the results presented here are preliminary, and are subject to change, some important qualitative conclusions can be drawn:

— E_{veto}, charged particle multiplicity, and E_T all depend strongly on impact parameter, making the selection of central collisions straightforward.

— The "central collision" peak in the E_T spectrum for ^{16}O projectiles can be described in position and width as a superposition of 16 p-nucleus central collisions.

— The value of E_T for central collisions between fairly asymmetric nuclei (^{16}O on Cu, Ag, Au) is proportional to $A_t^{1/3}$, i.e. E_T is proportional to the number of nucleons (about 50 for Au) in a tube in the target nucleus of diameter equal to that of the ^{16}O projectile.

— The multiplicity of positive particles for central collisions of ^{16}O on Pb (about 30) is consistent with this picture of the reaction geometry.

— The rapidity distributions for pions in central ^{16}O + Au collisions are centred on the c.m. of the 16+50 system rather than on that for p-p collisions.

— The angular distribution of pions in central ^{16}O + Au collisions is not isotropic in the c.m. system, and the transverse energy is of the order of 1/2 of that expected for an isotropic distribution.

— $\langle p_T \rangle$ for pions from central ^{16}O + Au collisions is the same as that for p-p collisions.

— The dependence of pion multiplicity on beam energy between 60 and 200 GeV/nucleon in central ^{16}O + Au collisions is consistent with that for p-p collisions over the same energy range.

— E_T in central ^{16}O + Au collisions roughly doubles between 60 and 200 GeV/nucleon and remains about the same proportion ($\sim 1/2$) of the available energy. There are no 60 GeV p-p data for comparison.

There are some results which present significant deviations from expectation, and which need to be explored further:

— The p_T distribution for negative particles, while having about the same $\langle p_T \rangle$, has a non-exponential shape, unlike that for p-p collisions or nucleus-nucleus models based on p-p collisions.

— The results of 2-pion interferometry suggest the presence of two sources, differing in size and chaoticity.

Since the energy density in ^{16}O + Pb collisions is found to be 2–3 GeV/fm^3, comparable to that predicted for production of a quark-gluon plasma, a continued intensive study of these collisions is worthwhile to look for evidence of such a phase transition. A number of important topics has not been mentioned in this report because the analysis is in too early a stage. These include:

— Study of the inclusive proton distributions to extract information on the systematics of nuclear "stopping power".

— Study of strange particles, which are recognized by their decay in the Streamer Chamber, and which have been suggested as a possible signature of a phase transition.

— Study of photon spectra, which are measured in the PPD: these have also been suggested as a probe of the quark-gluon plasma.

— Study of rapidity and azimuth fluctuations, to look for local production of the quark-gluon plasma or for deflagration phenomena. Such studies are very appropriate for the Streamer Chamber but do not have sufficient statistics at this stage of the measurement program.

5. Future projects

As indicated above, the analysis of the existing data is not complete, including that of some aspects which may provide information about the formation of the quark-gluon plasma. Among the present results the two-component p_T spectrum demands further study, while the two-pion correlations also seem a promising direction. An understanding of the increased isotropy of secondary particle emission compared with that observed in p-p

collisions should eventually provide a measure of nuclear "stopping power". Other experiments [13] at the SPS are investigating specific signals which are not studied in our experiment. These include target fragments (WA80), dimuons (NA34 and NA38), and multistrange baryons (NA36 and WA85). Any of a variety of smaller experiments could also produce a surprise.

The present data were produced in late 1986, and a second run will take place in Sept--Oct 1987 with ^{32}S beams. This will provide a challenge to the detectors, all the multiplicities being roughly doubled, and also an opportunity to test the systematics observed so far and suggested by various theories.

In the longer range future, the possibility exists of modifying the CERN facilities to accelerate Pb ions to 200 GeV/nucleon. Extrapolation from our present results suggests that an average energy density in excess of 4 GeV/fm^3 should be achieved for central collisions. However, experience at the Bevalac has indicated that ^{16}O (and even ^{32}S) are too small to make reasonable predictions of collective effects in large nuclei: experiment is essential.

A parallel program is underway at Brookhaven National Laboratory at the AGS. Experiments have already taken place with 14.5 GeV/nucleon ^{16}O and ^{32}Si. These should give important further indications on nuclear stopping, and provide information on a possible phase transition in the baryon-rich regime. By about 1990, BNL will have Au beams available in the same energy regime. Finally, a major colliding beam accelerator (RHIC) to collide 100 GeV/nucleon Au on 100 GeV/nucleon Au is in the last stages of approval for construction at Brookhaven. This could become available by about 1993, making energy densities in excess of 8 GeV/fm^3 over nuclear volumes of diameter 12 fm available for study [14].

In the more distant future, it seems likely that either CERN or the U.S.A., or both, will build a p-p collider with 10–20 TeV in each beam. A heavy ion source injecting into such a facility is estimated to produce an energy density in excess of 40 GeV/fm^3 [14].

This work was supported by the Director, Office of Energy Research, Division of Nuclear Physics of the Office of High Energy and Nuclear Physics of the U.S. Department of Energy under Contract DE-AC03-76SF00098.

REFERENCES

[1] J. B. Kogut, *Nucl. Phys.* **A418**, 381c (1984); H. Satz, *Nucl. Phys.* **A418**, 447c (1984).
[2] A. Sandoval et al., *Nucl. Phys.* **A461**, 465c (1987).
[3] M. Tincknell et al., Lawrence Berkeley Laboratory Report, LBL-22302 (1987).
[4] A. Bamberger et al., *Phys. Lett.* **B184**, 271 (1987).
[5] V. D. Aksinenko et al., *Nucl. Phys.* **A348**, 518 (1980).
[6] T. W. Ludlam, A. Pfoh, A. Shor, Brookhaven National Laboratory Report 51921, 373 (1985).
[7] J. D. Bjorken, *Phys. Rev.* **D27**, 140 (1983).
[8] T. Akesson et al., Proc. 23rd Internat. Conf. on High Energy Physics, Berkeley, California (1986); A. Franz, Ph. D. Thesis, Univ. Siegen 1986.
[9] This value is extrapolated from the data in W. Bell et al., *Z. Phys.* **A325**, 7 (1986).
[10] T. W. Atwater, P. S. Freier, J. I. Kapusta, Univ. of Minnesota preprint, Dec. 1986.

[11] T. Akesson et al., *Phys. Lett.* **B188**, 279 (1987).
[12] C. De Marzo et al., *Phys. Rev.* **D29**, 363 (1984), report source sizes and shapes for p-p and p-nucleus collisions at 200 GeV. However, their analysis procedure, which differs from the present one and from that of Ref. [11] is in doubt. See Ref. [11].
[13] Experiments at CERN in 1986, M. Ferro-Luzzi, CERN Research Board, 1986.
[14] These estimates are based on the energy dependence of p-p interactions, and probably represent a lower limit for nucleus-nucleus collisions.